Received: 1 January 2022, Accepted: 9 March 2022

Original Research

Journal of Advanced Veterinary Research
(2022) Volume 12, Issue 2, 99-106

Beak, Oropharyngeal and Nasal cavities of Broad Breasted White Turkey (*Meleagris gallopavo*): Gross Anatomical and Morphometrical Study

Fatma A. Madkour

Department of Anatomy and Embryology, Faculty of Veterinary Medicine, South Valley University, Qena 83523, Egypt.

Correspondence

Fatma A. Madkour, Department of Anatomy and Embryology, Faculty of Veterinary Medicine, South Valley University, Qena 83523, Egypt.
E-mail: madkour.f@vet.svu.edu.eg

Abstract

The anatomical description of the beak, oropharyngeal and nasal cavities of broad-breasted white turkey (BBWT) is unavailable in comparison with other birds. This study was conducted on five adult healthy birds (16.63 ± 5.54 Kg bwt). Beak was boat-shaped with pointed apex and was hard and rigid horny structure. The oral roof (palate) was formed of one median, two rostral, and two caudal palatine ridges. Shallow wide groove was observed between the rostral palatine ridges and lateral edges of the upper beak. The choanal slit was occupied 47.5% of the palate. There were two types of mechanical papillae distributed around the choanal slit. This slit was separated from the infundibular slit by a shallow groove. The tongue was triangular-shaped with pointed apex accompanied by V-shaped row of caudally directed lingual papillae between the body and the root. The lingual root was triangular-shaped, marked by shallow crescentic-shaped groove. The laryngeal mound was elongated pyramidal-shaped, contained glottis continued caudally by shallow longitudinal groove termed laryngeal sulcus. The nasal cavity was divided by a cartilaginous nasal septum into two symmetrical haves and opened externally by an elliptical-shaped nostril. The nostril was covered with a cartilaginous operculum which appeared as dome-shaped. Three nasal conchae were noticed within the nasal cavity: rostral, middle, and caudal nasal conchae. The middle nasal concha was the largest one, scrolled into 1 1/2 turns rostrally and scrolled 2 turns caudally. In conclusion, this study provides sufficient data on the anatomic and morphometric investigations of the nasal and oropharyngeal cavities of broad breast white turkey which may be beneficial for manipulation of head during treatment of diseases.

KEYWORDS
Beak, Broad Breasted White Turkey, Cavities, Slits, Tongue

INTRODUCTION

The domestic turkey (*Meleagris gallopavo domesticus*) were imported from central Mexico into Europe by the Spanish in the 16th century (Speller *et al*., 2010). Breeding of turkeys was acquired many developments in the early 20th century (Fuller, 2004). The turkey is a large bird of worldwide economic importance (Harvey *et al*., 1968). Broad Breasted White is commercially the most widely used breed of domesticated turkey. Because of their weight, which reached 30 kg, this bird predilection for overeating.

The mouth of the birds is bounded by horny upper and lower beaks, lead into oral and pharyngeal cavities (Evans, 1996). The former cavities are termed oropharynx as result of absence of soft palate, not that as in mammals (McLelland, 1975). Several authors have been interested in describing the oropharyngeal cavity of different avian species (Igwebuike & Eze, 2010; Abumandour, 2014; Sayed *et al*., 2016; Abumandour, 2018; Madkour, 2018; Abumandour & Gewaily, 2019; Madkour *et al*., 2019; Madkour *et al*., 2020; Madkour, 2020; Mahdy, 2020). This is due to the structural variations, which adapt the feeding habits and habitats. The characteristic features of the oropharynx may play a role on food intake and ingestion (Jayachitra *et al*., 2015). Additionally, the anatomical description of the avian nasal cavity is also taken the attention of some researchers (Ali, 2015; Casteleyn *et al*., 2018; Madkour, 2019; Dharani *et al*., 2020; Hanafy, 2021). The nasal cavity extends from nostril to choana, containing conchae and meatuses implying homology to those of mammals and other vertebrates (Bang & Wenzel, 1985). The nostrils of some birds are covered by an operculum (Harte, 1989). There are few published data on beak, oropharyngeal and nasal cavities of the turkey. The broad breasted white turkey (BBWT) has received little attention from anatomists in comparison with the other type of turkey such as broad breasted bronze. Thus, the anatomical study of the oropharyngeal cavity of broad breasted white turkey would be highly rewarding. To the best of the authors' knowledge, this study is the first one to highlight the anatomical and morphometrical investigations of upper and lower beaks, the oropharyngeal roof and floor of broad breasted white turkey in addition to nasal cavity. The current literature provides a first step towards the anatomical study of the digestive system of BBWT and compared it with the previously published data.

ISSN: 2090-6277/2090-6269/

MATERIALS AND METHODS

Birds and sample collection

This study was applied on five adults healthy broad breasted white turkeys of both sexes. These birds were collected from an international farm in Cairo, Egypt. The broad breasted white turkeys were sacrificed, and their heads were cut off after complete bleeding. The mean bodyweight of the turkeys was16.63 ± 5.54 Kg. The heads of these birds were rinsed in running water to get rid of any traces of blood. The beak's angles were incised laterally at the oral angles to open the mouth cavity wider for good exposure of the oropharyngeal cavity and fixed in 10% neutral buffered formalin (NBF). For the nasal cavity examination, it was undergone into two sections: sagittal section and cross-sections at the level of the rostral vestibular, middle respiratory, and caudal olfactory nasal regions

The slaughtering of the birds was performed following the animal ethical committee of the Faculty of Veterinary Medicine, SVU, Qena, Egypt. The terms were used in this study adoptino Nomina Anatomica Avium (Baumel *et al*., 1993).

Gross morphological examination

The gross morphological features of the beak, nasal, and oropharyngeal cavities were examined in detail using a magnification lens and were photographed using camera phone (Samsung Galaxy Note3).

Morphometrical and statistical analysis

The different measurements of the studied parts included the dimensions of: upper and lower beak, oropharyngeal roof and floor and its content as well as nasal cavity with its structures. These measurements were taken using Precision Digital Vernier Caliper (Vogel, Kevelaer, Germany) in millimeters. The data were expressed in the mean value ± standard deviation (SD) using Microsoft Office Excel 2016.

CMEIAS color segmentation

The figure of the cross-sections of the nasal cavity was converted to the negative images, performed as previously described by Madkour *et al*. (2022) and Madkour and Abdelsabour-Khalaf (2021).

RESULTS

Beak

The upper and lower beaks of BBWT were very hard and rigid, covered by horny keratin. Both beaks were off-white colored, boat-shaped with pointed apex. In addition, the lateral edges (tomium) of the beaks were smooth, very thin, and sharp. The upper beak (66.47±3.97 mm long) was supported by premaxilla bone, it was convex dorsally but concave ventrally. Its tip was located by 23.03±0.42 mm from the nostrils and 70.09±2.51 mm from the eyes. Furthermore, the height of the upper beak increased gradually caudally from its tip to the level of the caudal end of the nostril. The lower beak (61.84±2.08 mm long) was concave dorsally and slightly straight ventrally. The basis of the lower beak was formed by the mandible bone (Mandibula). The length of the mandibular body (Rostrum [Symphysis] mandibulae) and its width at the junction of the rami (Ramus mandibulae) were approximately similar. The width of the space between the mandibular rami was increased gradually by three folds at the level of the oral angles (Fig. 1A, B).

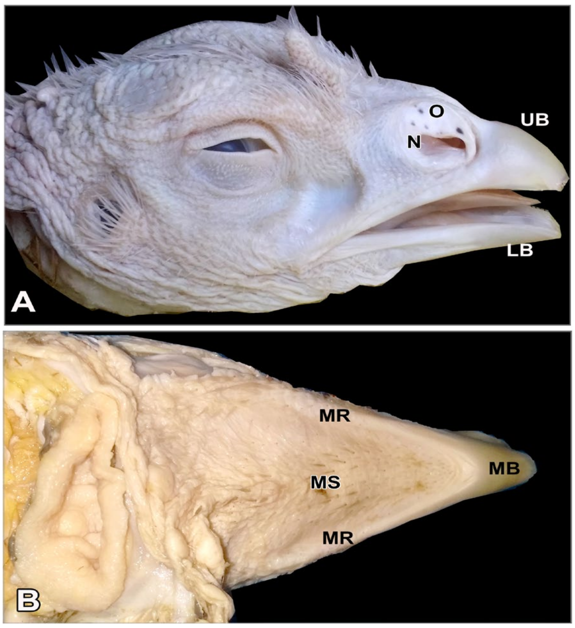

Fig. 1. Photographs of the beak of white broad breast turkey (WBBT). Showing upper beak (UB), lower beak (LL), mandibular body (MB), mandibular space (MS) between two rami (MR), nostril (N) covered by cartilaginous operculum (O).

Oropharyngeal cavity

The oropharyngeal cavity extended from the tip of the beak to the pharyngoesophageal junction. The oropharyngeal cavity was divided into the oropharyngeal roof and floor (Fig. 2A, B).

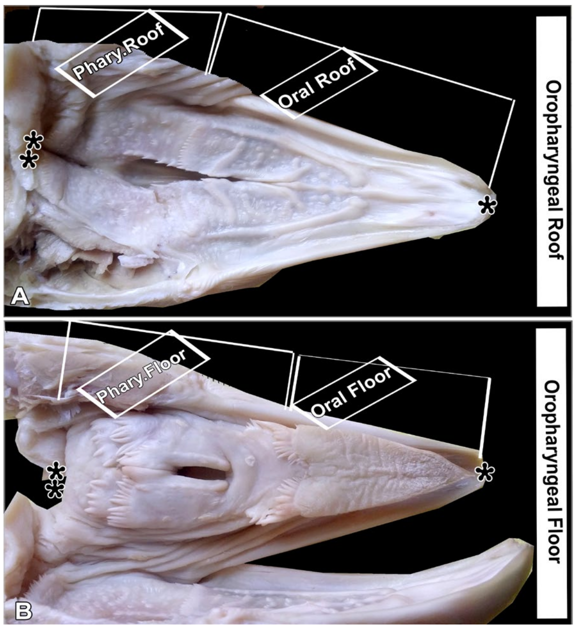

Fig. 2. Photographs of the oropharyngeal roof (A) and floor (B) of WBBT. Showing the extension of the oropharynx from tip of beak (star) to pharyngo-esophageal junction (double stars), extension of oral and pharyngeal roofs and floors.

Oropharyngeal roof

The oropharyngeal roof (101.82±3.39 mm long) was divided into oral and pharyngeal roofs. The line of separation between these roofs lied between the choanal and infundibular slits, which located behind the level of the angle of the mouth by 25.52±2.42 mm (Fig. 1A).

The oral roof represented the palate (Palatum), which was occupied by the choanal slit. Palate was triangular-shaped (80.49±1.30 mm long), divided into two parts: rostral and caudal parts. The line of demarcation between the former parts of the palate lied at the junction between the narrow rostral and wide caudal parts of the choanal slit (Fig. 3A, B).

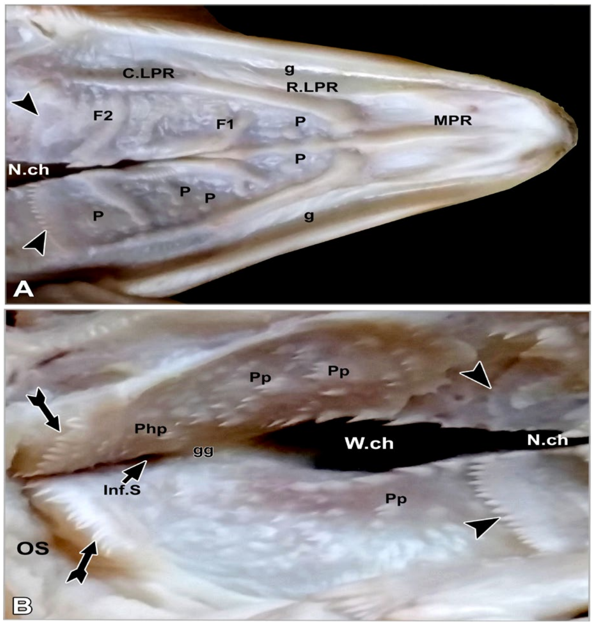

Fig. 3. Photographs of the oropharyngeal roof (A, B) of WBBT. Showing median palatine ridge (MPR), rostral palatine ridge (R.LPR), caudal palatine ridge (C.LPR), shallow wide groove (g), papillae (P), transverse folds (F1, F2), transverse row of caudally directed papillae (arrowheads) between the narrow (N.ch) and caudal (W.ch) parts of choanal slit, several caudally directed papillae (Pp) around wide part of choanal slit, pharyngeal papillae (Php), infundibular slit (Inf.s) separated from choanal slit by shallow grove (gg), transverse row of conical shaped papillae (barbed arrows) demarcated from oesophagus (OS).

All palatine ridges were concentrated at the rostral part of palate included: one median, two rostral, and two caudal palatine ridges. The median palatine ridge began behind the tip of the beak and terminated interruptedly at the rostral end of the choanal slit which continued at the level of the nasal septum. The rostral lateral palatine ridges extended at the same level of the beginning of the median one parallel and closed to the two caudal palatine ridges. The rostral palatine ridges were separated from the lateral edges of the beak by wide deep grooves. The two caudal lateral palatine ridges extended from the middle of the median one to terminate at the junction between narrow and wide parts of the choanal (at the end of the rostral part of the palate). The aforementioned ridges were approximately similar in length which recorded 44.36±3.65, 43.24±2.21, 44.36±3.65 mm for the median, rostral lateral, and caudal lateral palatine ridges, respectively (Fig. 3A).

The choanal slit (Choana) was formed of narrow rostral and wide caudal parts which occupied 47.5% of the palate. The rostral narrow part was longer, constituted 62.7% of the total length of the slit. Several papillae were distributed on each side of the slit. There were two types of mechanical papillae distributed around the choanal slit. The first was freely randomly distributed papillae; nodular-shaped papillae around the narrow part were increased in size and shape toward the wide part of the choanal slit. Most the papillae around the wide part were conical caudally directed with pointed apices and the others had a common basal part and bi-trifurcated into small papillae. While the second type was arranged in three transverse papillary rows. The first two rows appeared as folds extended from the edges of the slit to diverge laterally toward the caudal lateral palatine ridges while the third row consisted of conical caudally directed papillae at the junction between narrow and wide parts of the choanal slit. Moreover, few conical-shaped papillae were observed on the margins of the narrow part, becoming distinct papillary row on the wide part margins (Fig. 3A, B).

The pharyngeal roof (20.87±3.13 mm long) extended from the end of the choanal slit to the pharyngoesophageal junction. Elongated slit-like opening termed infundibular slit (Rima infundibuli) (10.24±1.13 mm) was occupied nearly 50% of the pharyngeal roof length. This slit separated from the choanal slit by shallow groove. Few small papillae were scattered on the pharyngeal surface which increased caudally toward the pharyngoesophageal junction. This junction was demarcated by well-marked transverse row papillae (Fig. 3B).

Oropharyngeal floor

The oropharyngeal floor (86.77±3.07 mm long) was formed of oral and pharyngeal floors. The row of the lingual papillae was the demarcation between them.

The oral floor was represented 58.72% of the oropharyngeal floor, it was occupied by the rostral two-third of the tongue (apex and body). The tongue (48.41±1.71 mm long) was triangular shaped with pointed apex and slightly increased in width caudally. The caudal end of the lingual body was forked and marked from the lingual root by V-shaped row of caudally directed lingual papillae which take the manner of the forked caudal fin of fish. The length of the caudally directed lingual papillae was increased lateralward, accompanied at the lateral ends by 4 papillae; two papillae with common stem on each side (Fig. 4A).

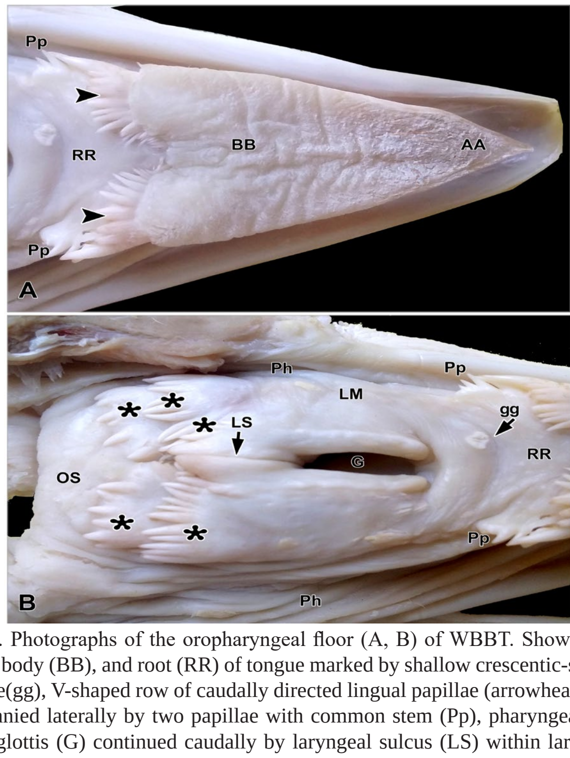

Fig. 4. Photographs of the oropharyngeal floor (A, B) of WBBT. Showing tip (AA), body (BB), and root (RR) of tongue marked by shallow crescentic-shaped groove(gg), V-shaped row of caudally directed lingual papillae (arrowheads) accompanied laterally by two papillae with common stem (Pp), pharyngeal wall (Ph), glottis (G) continued caudally by laryngeal sulcus (LS) within laryngeal mound (LM), two rows of caudally directed papillae (stars), oesophagus (OS).

The pharyngeal floor (35.76±5.07 mm) included the lingual root and laryngeal mound. The root was triangular-shaped, marked by shallow crescentic-shaped groove. It represented 16.15% of the total length of the tongue. The laryngeal mound was elongated pyramidal-shaped, its length was measured 34.81±1.07 mm while the width was 17.81±2.80 mm at the cranial end and 22.52±1.16 mm at the caudal end. The laryngeal mound contained an elongated opening called (glottis). The glottis was measured 11.41±0.53 mm long, marked by mucosal lips, and continued caudally by shallow longitudinal groove termed laryngeal sulcus (1.82±0.79 mm long). The caudal part of the laryngeal mound was marked from the pharyngoesophageal junction by two transverse rows of processes- like caudally directed papillae (Fig. 4B).

Nasal cavity

The nasal cavity of BBWT was elongated conical-shaped (51.76±3.53 mm long), it opened externally by an elliptical-shaped nostril, covered with a cartilaginous operculum (Fig. 5A). The length of the nostril was measured 15.73±1.47 mm long and 5.73±1.27 mm wide. From the dorsal surface of the upper beak, the operculum appeared as bulging dome-shaped (Fig. 5B). The rostral part of the rostral nasal concha enclosed the cartilaginous flap of the nostril which was shown through the opening of the nostril (Fig. 5C). Moreover, the nasal cavity was divided by a cartilaginous nasal septum into two symmetrical haves (Fig. 6A). Three nasal conchae were noticed within the nasal cavity: rostral, middle, and caudal nasal conchae. The rostral nasal concha was a kite-like, its rostral end could be seen within the nostril. The middle concha was the largest, an elongated-shaped with constriction at its middle part and located exactly above the level of the choanal slit. While the caudal nasal concha was the smallest inverted comma-shaped and occupied the caudal part of the nasal cavity above the dorsal surface of the middle concha (Fig. 6B). In cross-sections, the rostral concha was C-shaped surrounded cartilaginous flap of the nasal cartilage and projected within the nostril (Fig. 7A, B and 8A, B). While the middle concha (rostrally) was scrolled into 1 1/2 turns which curved dorsally, medially, then ventrally, and finally dorsally (Fig. 7C, D and 8C, D). At the level of the caudal olfactory region, the former concha was scrolled 2 turns (Fig. 7E, F and 8E, F). Moreover, the caudal concha was hollow mound-shaped, connected with the infraorbital sinus. The latter concha with the middle one were closely attached to the nasal septum (Fig. 7E, F and 8E, F).

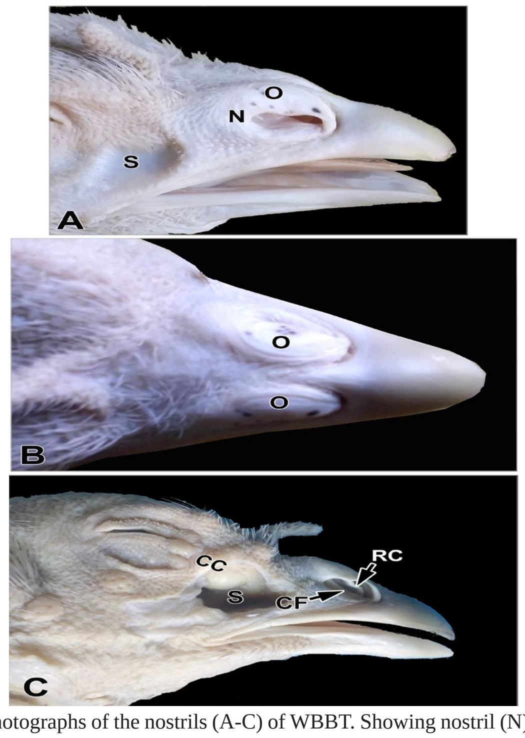

Fig. 5. Photographs of the nostrils (A-C) of WBBT. Showing nostril (N) covered by cartilaginous operculum (O), flap of nasal cartilage (CF) enclosed by rostral end of rostral concha (RC), infraorbital sinus (S), caudal nasal concha (CC).

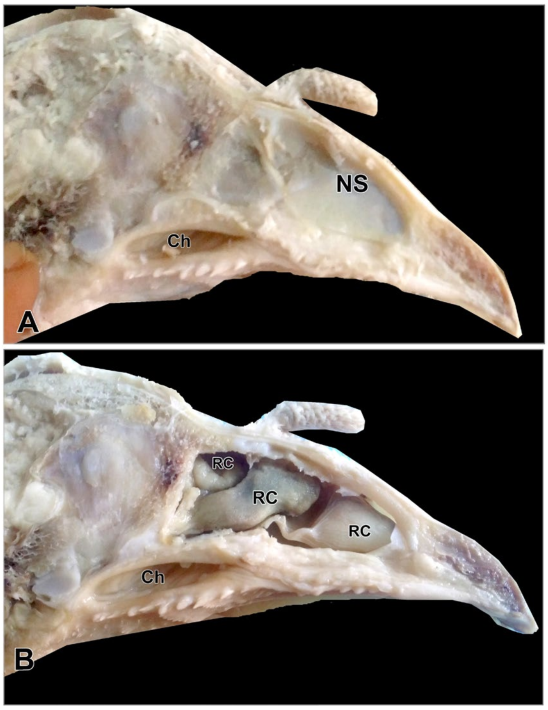

Fig. 6. Photographs of the sagittal section of the nasal cavity (A, B) of WBBT. Showing cartilaginous nasal septum (NS), choanal slit (Ch), rostral (RC), middle (MC) and caudal (CC) nasal conchae.

The infraorbital sinus in BBWT was well developed, measured 18.42±0.35 mm craniocaudally long. It was approximately rounded-shaped, located rostroventrally to the eyeball (Fig. 5C).
All morphometrical data of the oropharyngeal roof, floor, and nasal cavity were summarized in Tables 1, 2, and 3, respectively.

DISCUSSION

The beak form is related to the type of avian food and the means of food prehension. The type of food of the broad breast white turkey is dry so the beak was very hard and rigid, covered by horny keratin. These findings agree with the reports of Abumandour (2014) in Eurasian Hobby. While Abdalla *et al.* (2018) showed that the beak is soft in young ducks but hard in older ages ducks. The beak is totally soft in birds of family Charadriidae (Whittow, 2000). Additionally, the studied birds eat large amount of food by their beaks, so their shape take a shape of boat. In ostrich, the beak is flat spoon-shaped (Tajali *et al.*, 2008) and is curved in partridge (Rossi *et al.*, 2005). Furthermore, the obtained study as well as Crole and Soley (2010) in emu and Nickel *et al.* (1977) in fowl and pigeon revealed that the lateral edge of beak was smooth, very thin, and sharp. In contrast, Sayed *et al.* (2014) noted that the lateral edge of the beak of turkey has a serrate appearance due to the presence of transverse furrows. However, in duck, it is smooth laterally and lamellated medially (Abdalla *et al.*, 2018). These lamellae of the beak sieving the food particles from water. The inner aspect of the lower beak, has a median transverse ridge (Abumandour, 2014) in Eurasian Hobby and (Crole & Soley, 2010) in emu.

The economic loss of the turkey industry usually occurs as result of diseases of the respiratory system, particularly the nasal cavity. For example, the common respiratory disease of the turkey is the infectious sinusitis caused by Mycoplasma gallisepticum (Hennigan *et al.*, 2012). Despite, the anatomical study of the cavities within the head of the different types of turkey especially the nasal cavity not interested in anatomists. So, this study provides sufficient data about the anatomic and morphometric investigations of the nasal and oropharyngeal cavities of BBWT. Whilst further studies like 3D computed tomography of turkey head are required to have a complete available data that will be used in detection the treatment of the sinusitis.

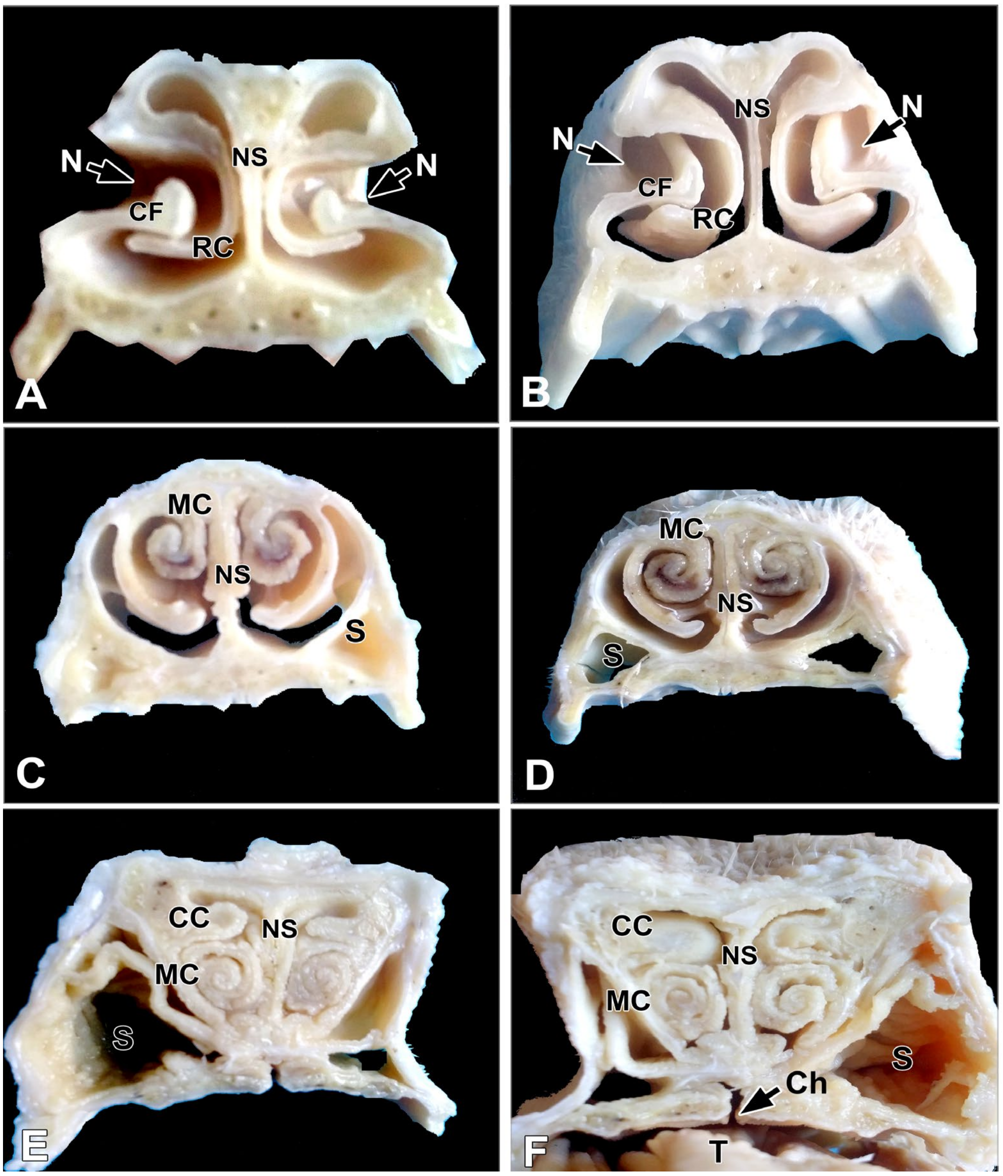

Fig. 7. Photographs of the cross section of the nasal cavity (A, B) at the level of the rostral vestibular region, (C, D) at the level of middle respiratory region, (E, F) at the level of the caudal olfactory region of WBBT. Showing nasal septum (NS), nostril (N), flap of nasal cartilage (CF), rostral (RC), middle (MC), and caudal (CC) nasal conchae, infraorbital sinus (S), choanal slit (Ch), lingual body (T).

Table 1. Morphometrical measurements (in mm) of the oropharyngeal roof

Dimensions	Mean	SD
Oral roof		
– Total length of oropharyngeal roof	101.82	3.39
– Length of oral roof (palate**)**	80.49	1.3
– Distance between line of transition of oral & pharyngeal cavities and angle of mouth	25.52	2.42
– Length of median palatine ridge	44.36	3.65
– Length of rostral lateral palatine ridge	43.24	2.21
– Length of caudal lateral palatine ridge	44.36	3.65
– Distance between median palatine ridge and tip f beak	8.28	1.4
Choanal slit		
– Total length of choanal slit	38.31	0.49
– Length of narrow part	24.04	1.42
– Length of wide part	14.27	1.39
Pharyngeal roof:		
– Length of pharyngeal roof	20.87	3.13
Infundibular slit:		
– Length	10.24	1.13

Table 2. Morphometrical measurements (in mm) of the oropharyngeal floor

Dimensions	Mean	SD
Oral floor		
– Total length of oropharyngeal floor	86.77	3.07
– Length of oral floor	50.96	2.3
Pharyngeal floor		
– Length of pharyngeal floor	35.76	5.07
Tongue		
– Total length of tongue:	48.41	1.71
Length of		
– Apex	31.83	0.06
– Body	8.75	0.6
– Root	7.82	1.03
Width of tongue		
– At level of frenulum linguae	19.62	0.17
– At level of transverse row of papillae	20.57	0.52
Laryngeal mound		
Length of		
– Laryngeal mound	34.81	1.07
– Laryngeal inlet (glottis)	11.41	0.53
– Laryngeal sulcus	1.82	0.79
Width of:		
– Laryngeal mound at its cranial end	17.81	2.3
– Laryngeal mound at its caudal end	22.52	1.16
– Laryngeal inlet (glottis)	3.11	0.83

Table 3. Morphometrical measurements (in mm) of the nasal cavity

Dimensions	Mean	SD
Length of nasal cavity	51.76	3.53
Length of nasal conchae		
– Rostral nasal concha	29.18	2.07
– Middle nasal concha	30.87	2.48
– Caudal nasal concha	11.03	0.56
Nostril		
– Length	15.73	1.47
– Width	5.73	1.27
Length of infraorbital sinus	18.42	0.35

The current study agrees with the previous published data (Nickel *et al*., 1977; Mohamed & Zayed, 2003; Jayachitra *et al*., 2015; Sayed *et al*., 2016; Madkour, 2018) that the palate formed of median and lateral palatine ridges with variable terminations as reported from the obtained literature. Concerning the median palatine ridge was terminated interruptedly at the rostral end of the choanal slit, this result is nearly similar with the reports of Sayed *et al*. (2016) in turkey and Ali (2004) in ostrich. In this connection, the oral roof of goose has median longitudinal palatine ridge and 2-3 paramedian rows (Mohamed & Zayed, 2003). On the other hand, emu has one median palatine ridge only (Crole & Soley, 2011). The palatine ridges play role with other palatine papillae in transportation of the bolus toward the esophagus.

The reports of Madkour (2018) in quail and dove supported our findings that the groove extended between the edges of upper beak and lateral palatine ridges allow to passage the grains toward the pharynx and also grip the closure of the beak. Regarding the morphometrical analysis, the palate formed 79.05% of the total length of the oropharyngeal roof. Nearly the same percentage has been recorded in pigeon and goose (Mohamed & Zayed, 2003), and it is 87.09% in young and 88.03% in adult pigeon (Mahdy, 2020), 71.26% in turkey (Gupta *et al*., 2015), 86% in dove and 73% in quail (Madkour, 2018).

The obtained observations agree with the findings of Madkour (2018), Madkour *et al*. (2019), and Sayed *et al*. (2017) that the choanal slit was completely located at the palate in front the infundibular slit. We noticed shallow groove between these slits and the distance between them is 3 mm in chicken and 6 mm in goose (Mohamed & Zayed, 2003). However, two slits are opened together in the budgerigar (Evans, 1996).

The distribution of the papillae around the choanal slit differs among avian species depending on their feeding habits which prevent entrance any debris into the nasal cavity. These papillae were distributed by two types around choanal slit of BBWT; the first type was freely randomly distributed papillae and the second arranged in three transverse papillary rows, in addition to few papillae on the narrow part edges and one papillary row on the wide part edges. The papillae are observed only on the margins of the narrow part of the slit in pigeon (Mahdy, 2020), hoopoe (Abumandour & Gewaily, 2019), and the papillae are distributed in 2 longitudinal rows on the edges of the wide part (Madkour *et al*., 2019) in duck. On the other hand, the papillae surrounding the slit are completely absent in laughing dove (Madkour, 2018) and emu (Crole & Soley, 2010).

The tongue of birds is a species-specific because of its morphological characterizations depending on the different lifestyles, feeding habits and habitats (Onuk *et al*., 2013; Erdoğan & Iwasaki, 2014). The avian lingual shape is closely related to the form of the lower beak and feeding habits of the different avian species (Nickel *et al*., 1977). The shape of the studied tongue was triangular adapted to the concavity of the lower beak which is considered the general form of the avian tongue as mentioned by many authors (Jackowiak *et al*., 2010; Parchami *et al*., 2010; Abumandour, 2018; Abumandour & Gewaily, 2019). There is another lingual shape such as elongated oval-shaped in coot (Abumandour & El-Bakary, 2017), elongated in white-tailed eagle (Jackowiak & Godynicki, 2005), and a needle-like in Egret, black-crowned night heron and green-backed heron (Emura, 2009).

The obtained study as well as Dehkordi *et al*. (2010) in zebra finch, and El-Bakary (2011) in hoopoe showed that the lingual apex was pointed. It is round flat in goose, duck and quail (Emura, 2009), bifid in house sparrow (Abumandour, 2018), and in Eurasian Hobby (Abumandour, 2014). Furthermore, Abumandour and El-Bakary (2017) noticed characterized feature on the rostral end of the lingual apex of coot which carries multiple long, rostrally directed processes. The avian lingual apex play role in collection, manipulation of foods so its shape is various according feeding habits and type of food.

In the present study, the description of the laryngeal mound matches with previously published reports, which is a raised structure located caudal to the lingual root (Abumandour, 2014; Madkour, 2018; Mohamed *et al*., 2018). Additionally, at the caudal part laryngeal mound, two transverse rows of caudally directed papillae were noticed as mentioned by Dyce *et al*. (2002) and Abumandour (2014), but one row in dove and three rows in quail (Madkour, 2018). Whilst, numerous irregular distributed papillae occupied the caudal part of the laryngeal mound (Mohamed *et al*., 2018).

Avian nostrils are covered by various structures or non-covered based on the habitats, lifestyle, species of the birds. In our observations, the covering of the opening of the nostril of BBWT was cartilaginous operculum, but is horny structure in quail and dove (Madkour, 2019), osseous tubercula in falcon to slow down the passage of the air into the nostrils (Stettenheim, 2000), and a tuft of feathers in hooded crow (Hassan, 2012). On the other hand, some birds have un-covered nostrils as in ostrich (Ali, 2015) and duck, goose (Madkour, 2019).

Generally, the nasal conchae within nasal cavity are conditioning of the inhaled air (Geist, 2000), and also increase the surface

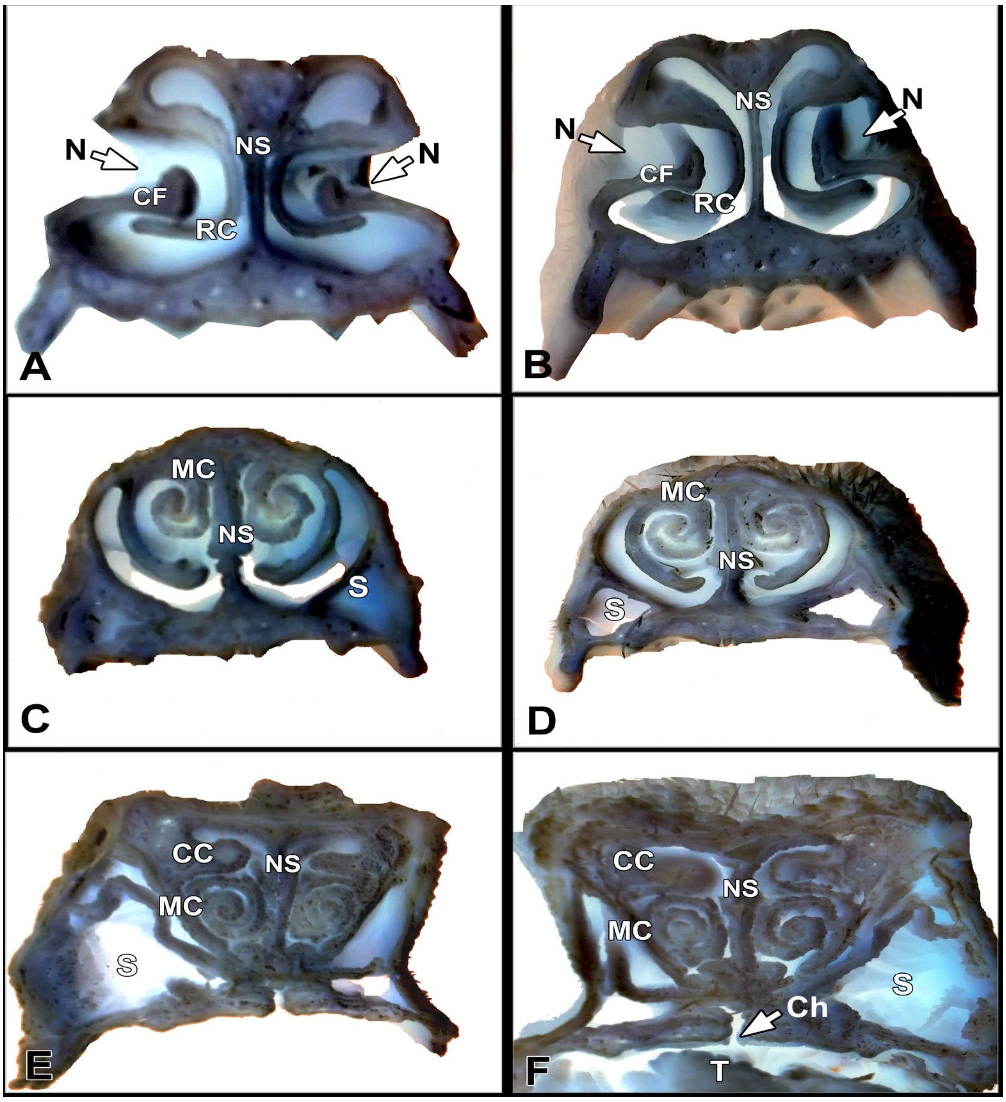

Fig. 8. Photographs of the cross section of the nasal cavity (A, B) at the level of the rostral vestibular region, (C, D) at the level of the middle respiratory region, (E, F) at the level of the caudal olfactory region of WBBT. Showing the Negative image of Figure 7 to clarify. Nasal septum (NS), nostril (N), flap of nasal cartilage (CF), rostral (RC), middle (MC), and caudal (CC) nasal conchae, infraorbital sinus (S), choanal slit (Ch), lingual body (T).

area of the cavity (Danner *et al.*, 2017). Concerning the number of nasal conchae, the current study agrees with reports of Hanafy (2021) in moorhen, Madkour (2019) in duck, goose, quail, Ali (2015) and Jin *et al.* (2008) in ostrich who mention that the nasal cavity has three nasal conchae (rostral, middle, and caudal). Contrarily, two conchae (rostral and caudal) are noticed in dove (Madkour, 2019), hooded crow (Hassan, 2012), and common moorhen (Khazaalwaad *et al.*, 2020). However, the absence of nasal conchae is reported by Schmidt *et al.* (2015) in parrot. The cross sections of the nasal cavity showed that the middle nasal concha scrolled into 11/2 turns rostrally and 2 turns caudally. The scrolling of the middle concha at the rostral part resembled that reported in duck (Madkour, 2019) and in moorhen (Hanafy, 2021), while the scrolling at the caudal part of the middle concha as that mentioned in goose (Madkour, 2019). The scrolling of the nasal conchae allows a good humidification of the inhaled air. In agreement with Hanafy (2021) in moorhen who noticed that the infraorbital sinus is rounded shaped, but it is large triangular-shaped in duck and goose, and small triangular-shaped in quail and dove (Madkour, 2019).

CONCLUSION

This study provides, for the first time, comprehensive information on the anatomy and morphometry of the beak, nasal and oropharyngeal cavities of broad breast white turkey (BBWT). Further studies are required to have a complete local atlas for the anatomy of this bird.

ACKNOWLEDGMENTS

The author is thankful to veterinarian Nagwa Madkour for her help to provide sufficient birds to complete this study.

CONFLICT OF INTEREST

The author declare that no conflict of interest exists.

REFERENCES

Abdalla, K., Mohamed, S., Madkour, F., 2018. Histomorphogenesis of Upper Beak in Muscovy Ducks (*Cairina moschata*). SVU-International Journal of Veterinary Sciences 1, 12-24.

Abumandour, M., El-Bakary, N., 2017. Morphological characteristics of the oropharyngeal cavity (tongue, palate and laryngeal entrance) in the Eurasian coot (*Fulica atra*, Linnaeus, 1758). Anatomia, histologia, embryologia 46, 347-358.

Abumandour, M.M., 2014. Gross anatomical studies of the oropharyngeal cavity in Eurasian hobby (Falconinae: *Falco Subbuteo*, Linnaeus 1758). Journal of Life Sciences Research 1, 80-92.

Abumandour, M.M., 2018. Surface ultrastructural (SEM) characteristics of oropharyngeal cavity of house sparrow (*Passer domesticus*). Anatomical science international 93, 384-393.

Abumandour, M.M., Gewaily, M.S., 2019. Gross morphological and ultrastructural characterization of the oropharyngeal cavity of the Eurasian hoopoe captured from Egypt. Anatomical science international 94, 172-179.

Ali, S., 2015. Gross anatomical studies on the nasal cavity of the ostrich. Benha Veterinary Medical Journal 29, 326-332.

Ali, S. A.M., 2004. Some morphological studies on the oropharynx of the ostrich (*Struthio camelus*). Thesis, M.Sc. Menoufyia University, Egypt.

Bang, B., Wenzel, B., 1985. Nasal cavity and olfactory system. Form and function in birds 3, 195-225.

Baumel, J.J., King, S.A., Breazile, J.E., Evans, H.E., Berge, J.C.V., 1993. Handbook of avian anatomy: Nomina anatomica avium (2nd Ed.).Cambridge: Nuttall Ornithological Club 779p.

Casteleyn, C., Cornillie, P., Van Cruchten, S., Van den Broeck, W., Van Ginneken, C., Simoens, P., 2018. Anatomy of the upper respiratory tract in domestic birds, with emphasis on vocalization. Anatomia, histologia, embryologia 47, 100-109.

Crole, M., Soley, J., 2010. Gross morphology of the intra-oral rhamphotheca, oropharynx and proximal oesophagus of the emu (*Dromaius novaehollandiae*). Anatomia, histologia, embryologia 39, 207-218.

Crole, M.R., Soley, J.T., 2011. Distribution and structure of glandular tissue in the oropharynx and proximal esophagus of the emu (*Dromaius novaehollandiae*). Acta Zoologica 92, 206-215.

Danner, R.M., Gulson-Castillo, E.R., James, H.F., Dzielski, S.A., Frank III, D.C., Sibbald, E.T., Winkler, D.W., 2017. Habitat-specific divergence of air conditioning structures in bird bills. The Auk: Ornithological Advances 134, 65-75.

Dehkordi, R.A.F., Parchami, A., Bahadoran, S., 2010. Light and scanning electron microscopic study of the tongue in the zebra finch Carduelis carduelis (Aves: Passeriformes: Fringillidae). Slovenian Veterinary Researcha 47, 139-144.

Dharani, P., Kannan, T., Devi, R.G., Ramesh, G., Balasubramanian, S., Pazhanivel, N., 2020. Nasal conchae in Nandanam chicken-gross, histological and immunohistochemical study. Pakistan Veterinary Journal 40, 514-518.

Dyce, K., Sack, W., Wensing, C., 2002. Textbook of Veterinary Anatomy. Philadelphia, PA: Saunders. Inc.

El-Bakary, N.E., 2011. Surface morphology of the tongue of the hoopoe (*Upupa epops*). Journal of American Science 7, 394-399.

Emura, S., 2009. SEM studies on the lingual dorsal surfaces in three species of herons. Medicine and Biology 153, 423-430.

Erdoğan, S., Iwasaki, S., 2014. Function-related morphological characteristics and specialized structures of the avian tongue. Annals of Anatomy-Anatomischer Anzeiger 196, 75-87.

Evans, H.E., 1996. Anatomy of the budgerigar and other birds. In: Diseases of Cage and Aviary Birds (RossKopf, W. J.; Woerpel, R.W., eds). (3rd Ed.). Philadelphia: Lea & Febiger, williams & wilkins a waverly company.

Fuller, M.F., 2004. The encyclopedia of farm animal nutrition. Cabi.

Geist, N.R., 2000. Nasal respiratory turbinate function in birds. Physiological and Biochemical Zoology 73, 581-589.

Gupta, S. K., Archana, P., Farooqui, M., 2015. Anatomy of oropharyngeal cavity of fowl (*Gallus domesticus*). Indian Journal of Veterinary Anatomy 27, 12-14.

Hanafy, B. G., 2021. Structural adaption of the nasal conchae of Eurasian common moorhen (*Gallinula chloropus chloropus*, Linnaeus, 1758)—Histomorphological study. Microscopy research and technique.

Harte, J., 1989. The Birder's Handbook: A Field Guide to the Natural History of North American Birds. BioScience 39, 492-494.

Harvey, E. B., Kaiser, H. E., Rosenberg, L. E., 1968. An atlas of the domestic turkey (*Meleagris gallopavo*): myology and osteology. 7, US Atomic Energy Commission, Division of Biology and Medicine.

Hassan, S., 2012. Gross anatomical features of the nasal cavity of the hooded crow (Corvuscornix). Suez Canal University Medical Journal 17, 119-127.

Hennigan, S. L., Driskell, J. D., Ferguson-Noel, N., Dluhy, R. A., Zhao, Y., Tripp, R. A., Krause, D. C., 2012. Detection and differentiation of avian mycoplasmas by surface-enhanced Raman spectroscopy based on a silver nanorod array. Applied and environmental microbiology 78, 1930-1935.

Igwebuike, U. M., Eze, U. U., 2010. Anatomy of the oropharynx and tongue of the African pied crow (*Corvus albus*). Veterinarski arhiv 80, 523-531.

Jackowiak, H., Godynicki, S., 2005. Light and scanning electron microscopic study of the tongue in the white tailed eagle (*Haliaeetus albicilla*, Accipitridae, Aves). Annals of Anatomy-Anatomischer Anzeiger 187, 251-259.

Jackowiak, H., Skieresz-Szewczyk, K., Kwieciński, Z., Trzcielińska-Lorych, J., Godynicki, S., 2010. Functional morphology of the tongue in the nutcracker (*Nucifraga caryocatactes*). Zoological Science 27, 589-594.

Jayachitra, S., Balasundaram, K., Iniyah, K., Sivagnanam, S., Tamilselvan, S., 2015. Morphology of oropharyngeal cavity in guinea fowl (*Numida meleagris*). International Journal of Advanced Multidisciplinary Research 2, 99-102.

Jin, E., Peng, K., Wang, J. A., Du, A., Tang, L., Wei, L., Song, H., 2008. Study of the morphology of the olfactory organ of African ostrich chick. Anatomia, histologia, embryologia 37, 161-165.

Khazaalwaad, S., Mohamed, A. A., Arean, A. G., Hashim, W. S., 2020. Morphological and histological study of concha in moorhen (Gallinula). International Journal of Psychosocial Rehabilitation 24, 5718-5722.

Madkour, F., 2018. Characteristic features of the pharyngeal cavity of the laughing dove (*Streptopelia senegalensis aegyptiaca*) and Japanese quail (*Coturnix coturnix*). Assiut Veterinary Medical Journal 64, 52-59.

Madkour, F., Abdalla, K., Mohamed, S., 2019. Choana morphogenesis in developmental stages of Muscovy ducks. SVU-International Journal of Veterinary Sciences 2, 13-26.

Madkour, F., Abdalla, K. E., Mohamed, S. A., 2020. Histomorphogenesis of the Pharyngeal roof in Muscovy Ducks (*Cairina moschata)*. SVU-International Journal of Veterinary Sciences 3, 106-114.

Madkour, F., Abdelsabour-Khalaf, M., 2021. Gross anatomical and morphometrical study of the nasal cavity (cavum nasi) of Egyptian goat (Capra hircus) and Egyptian Baladi dog (Canis lupus). SVU-International Journal of Veterinary Sciences 4, 80-93.

Madkour, F. A., 2018. Morphological studies of the oral roof of the Egyptian laughing dove (*Streptopelia senegalensis aegyptiaca*) and Japanese quail (*Coturnix coturnix japonicum*). Journal of Veterinary Anatomy 11, 17-39.

Madkour, F. A., 2019. Anatomical descriptions of the nasal cavity of the aquatic and non-aquatic birds. SVU-International Journal of Veterinary Sciences 2, 101-110.

Madkour, F. A., 2020. Comparative Histology and Micrometric Analysis of Pharyngeal cavity in Egyptian Laughing Dove (*Streptopelia senegalensis aegyptiaca*) and Japanese Quail (*Coturnix coturnix japonicum*). SVU-International Journal of Veterinary Sciences 3, 115-129.

Madkour, F. A., Mohamed, S. A., Abdalla, K. E. H., Ahmed, Y. A., 2022. Developmental stages and growth of the proventriculus of post-hatching Muscovy duck: Light and electron microscopic study. Microscopy research and technique 85, 56–70.

Mahdy, M. A., 2020. Comparative gross and scanning electron microscopical study of the oropharyngeal roof of young and adult domestic pigeons (*Columba livia domestica*). Microscopy research and technique 83, 1045-1055.

McLelland, J., 1975. Aves digestive system. In: Sisson and Grossman's The Anatomy of the Domestic Animals (Getty, R.,ed.) (Vol. 2, 5th Ed.). Philadelphia and London: W. B. Saunders Co. pp. 1857-1865.

Mohamed, S., Zayed, A., 2003. Gross anatomical and scanning electron microscopical studies on palate of some birds. Assiut Veterinary Medical Journal 49, 1-17.

Mohamed, S. A., Abdelsabour-Khalaf, M., Abdelhakeem, F., 2018. Morphological characterization of the laryngeal mound of the Egyptian geese. Assiut Veterinary Medical Journal 64, 1-8.

Nickel, R., Schummer, A., Seiferle, E., 1977. Anatomy of the domestic birds. Berlin: Hamburg: Verlag Paul Parey.

Onuk, B., Tütüncü, S., Kabak, M., Alan, A., 2013. Macroanatomic, light microscopic, and scanning electron microscopic studies of the tongue in the seagull (L *arus fuscus*) and common buzzard (*Buteo buteo*). Acta Zoologica 96, 60-66.

Parchami, A., Dehkordi, R. F., Bahadoran, S., 2010. Fine structure of the dorsal lingual epithelium of the common quail (*Coturnix coturnix*). World Applied Sciences Journal 10, 1185-1189.

Rossi, J. R., Baraldi-Artoni, S. M., Oliveira, D., Cruz, C. d., Franzo, V. S., Sagula, A., 2005. Morphology of beak and tongue of partrigde Rhynchotus rufescens. Ciência Rural 35, 1098-1102.

Sayed, R. K., Abdalla, K. E., Ahmed, A. K., Saleh, A. M., 2014. Morphological studies on the upper beak of Turkey (*Meleagris gallopavo*). Journal of Advanced Veterinary Research 4, 154-160.

Sayed, R. K., Abdalla, K. E., Ahmed, A. K., Saleh, A. M., 2016. Palate of Turkey (*Meleagris gallopavo*): Gross anatomical, light and scanning electron microscopical study. Journal of Advanced Veterinary Research 6, 81-88.

Sayed, R. K., Abdalla, K. E., Saleh, A. M., Ahmed, A. K., 2017. Macro and microanatomical studies on the choanal slit of Turkey (*Meleagris gallopavo*). Journal of Advanced Veterinary Research 7, 75-80.

Schmidt, R. E., Reavill, D. R., Phalen, D. N., 2015. Pathology of pet and aviary birds. John Wiley & Sons.

Speller, C. F., Kemp, B. M., Wyatt, S. D., Monroe, C., Lipe, W. D., Arndt, U. M., Yang, D. Y., 2010. Ancient mitochondrial DNA analysis reveals complexity of indigenous North American turkey domestication. Proceedings of the National Academy of Sciences 107, 2807-2812.

Stettenheim, P. R., 2000. The integumentary morphology of modern birds—an overview. American Zoologist 40, 461-477.

Tajali, M., Mansouri, S. H., Poust, P. A., 2008. Gross anatomy of the oropharyngeal cavity in the ostrich (*Struthio camelus*). Iranian Journal of Veterinary Research 9, 316-323.

Whittow, G. C., 2000. Sturkies African Physiology (5th Ed.). Academic Press, USA. pp. 299-325.